nature structural & molecular biology

LIN-28 and the poly(U) polymerase PUP-2 regulate let-7 microRNA processing in *Caenorhabditis elegans*

Nicolas J Lehrbach[1,2,5], Javier Armisen[1,2,5], Helen L Lightfoot[1,3], Kenneth J Murfitt[1], Anthony Bugaut[3], Shankar Balasubramanian[3,4] & Eric A Miska[1,2]

The let-7 microRNA (miRNA) is an ultraconserved regulator of stem cell differentiation and developmental timing and a candidate tumor suppressor. Here we show that LIN-28 and the poly(U) polymerase PUP-2 regulate let-7 processing in *Caenorhabditis elegans*. We demonstrate that *lin-28* is necessary and sufficient to block *let-7* activity *in vivo*; LIN-28 directly binds let-7 pre-miRNA to prevent Dicer processing. Moreover, we have identified a poly(U) polymerase, PUP-2, which regulates the stability of LIN-28–blockaded let-7 pre-miRNA and contributes to LIN-28–dependent regulation of let-7 during development. We show that PUP-2 and LIN-28 interact directly, and that LIN-28 stimulates uridylation of let-7 pre-miRNA by PUP-2 *in vitro*. Our results demonstrate that LIN-28 and let-7 form an ancient regulatory switch, conserved from nematodes to humans, and provide insight into the mechanism of LIN-28 action *in vivo*. Uridylation by a PUP-2 ortholog might regulate let-7 and additional miRNAs in other species. Given the roles of Lin28 and let-7 in stem cell and cancer biology, we propose that such poly(U) polymerases are potential therapeutic targets.

Small RNAs regulate gene expression in many eukaryotes, including plants, animals and fungi. miRNAs are endogenous short RNAs that modulate gene expression by blocking translation and/or destabilizing target mRNAs[1,2]. In animals, miRNAs are transcribed as long precursors (pri-miRNAs) that are processed in the nucleus by the RNase III enzyme complex Drosha–Pasha–DGCR8 to form ~80-nt pre-miRNAs, or are derived directly from introns[3]. pre-miRNAs are exported from the nucleus and processed by the RNase III enzyme Dicer and then incorporated into an Argonaute-containing RNA-induced silencing complex (RISC). The first identified miRNAs, the products of the *C. elegans* genes *lin-4* and *let-7*, control cell fates during larval development[4]. When either *lin-4* or *let-7* is inactivated, specific epithelial cells fail to differentiate and undergo additional divisions. lin-4 acts during early larval development, regulating *lin-14* and *lin-28* mRNAs[4–8]. let-7 acts during late larval development, regulating *lin-41*, *hbl-1*, *daf-12* and *pha-4* mRNAs[9–12]. As such, the time of appearance of these miRNAs must be tightly controlled. In *C. elegans* and other animals, the expression of let-7 is developmentally regulated, but the mechanisms underlying this regulation remain unknown[13]. Post-transcriptional regulation of specific miRNAs has recently been uncovered[14]. let-7 biogenesis is blocked by Lin28 at either the Drosha[15,16] or the Dicer[17,18] step in mammalian cell culture. Lin28 is a conserved RNA-binding protein that, in mammals, controls stem cell lineages and inhibits let-7 miRNA processing *in vitro*[15–19]. However, the mechanism and *in vivo* significance of this activity are unclear. We therefore set out to examine post-transcriptional regulation of let-7 in *C. elegans*.

RESULTS

let-7 activity is developmentally regulated in *C. elegans*

To study the mechanism of miRNA action *in vivo*, we established a quantitative miRNA reporter assay based on let-7 in *C. elegans* (**Fig. 1a,b** and **Supplementary Methods**). We generated two transgenes comprising the promoter of *myo-2*, the coding sequences of either green fluorescent protein (GFP) or mCherry and the 3′ untranslated region (UTR) of either *lin-41* or *unc-54* (*myo-2::gfp::lin-41* and *myo-2::mcherry::unc-54*; hereafter referred to as the 'let-7 sensor'; **Fig. 1a**). The *myo-2* promoter confers expression exclusively in the pharyngeal muscle, which is the food pump of *C. elegans*[20]; *lin-41* is a genetically identified target of the let-7 miRNA[9], whereas the *unc-54* 3′ UTR is not known to be regulated by any miRNA.

Transgenic animals carrying an intrachromosomal array of the let-7 sensor expressed both GFP and mCherry strongly throughout larval development (**Fig. 1c**). As expected, in animals that also carried a transgene expressing let-7 (*myo-2::let-7*), silencing of GFP, but not of mCherry, was observed (**Fig. 1d**). Unexpectedly, this effect was developmentally regulated; inhibition of GFP is markedly stronger in adults than in L1 larvae (**Fig. 1d**). As the *let-7* transgene does not contain the *let-7* promoter, this regulation must occur post-transcriptionally. In addition to the qualitative analysis of fluorescent protein expression using microscopy, we quantified the activity of the let-7 sensor using flow cytometry of whole animals. We used a COPAS Biosort instrument to quantify GFP and mCherry expression along the body axis of thousands of individual animals at different stages during development. Silencing of the let-7 sensor was least efficient at the L1 larval stage and reached maximal efficiency during L3 (**Supplementary Fig. 1**

[1]Wellcome Trust Cancer Research UK Gurdon Institute, University of Cambridge, The Henry Wellcome Building of Cancer and Developmental Biology, Cambridge, UK. [2]Department of Biochemistry, [3]Department of Chemistry and [4]School of Clinical Medicine, University of Cambridge, Cambridge, UK. [5]These authors contributed equally. Correspondence should be addressed to E.A.M. (eam29@cam.ac.uk).

Received 18 August; accepted 20 August; published online 27 August 2009; doi:10.1038/nsmb.1675

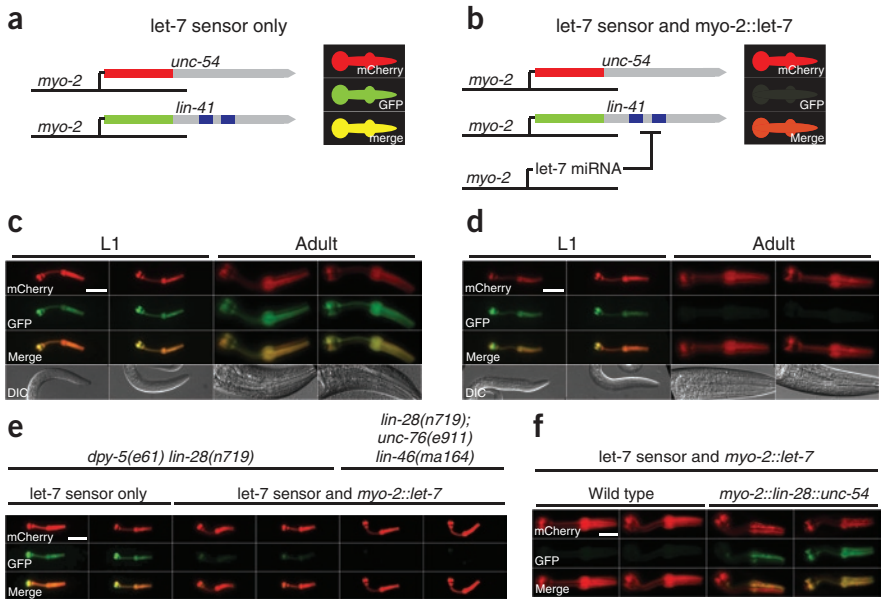

Figure 1 A quantitative assay reveals post-transcriptional regulation of the let-7 miRNA by LIN-28. (**a**,**b**) Schematic of the pharynx-based assay of let-7 activity. (**c**) Fluorescence images of animals carrying the let-7 sensor transgene at L1 larval and adult stages. Both GFP and mCherry are strongly expressed. (**d**) Fluorescence images of animals carrying both the let-7 sensor and *myo-2::let-7* transgenes at L1 larval and adult stages. GFP is specifically and robustly downregulated in adults, but not in L1 larvae. Scale bar shows 20 μm. (**e**) Fluorescence images showing that *lin-28* mutants downregulate let-7 sensor GFP at the L1 stage in a *myo-2::let-7*–dependent fashion. This effect is not reversed in a *lin-46* mutant background. Scale bar shows 20 μm. (**f**) Fluorescence images showing that a *myo-2::lin-28::unc-54* transgene is sufficient to block let-7 activity in adults carrying let-7 sensor and *myo-2::let-7* transgenes. Scale bar shows 20 μm.

and **Supplementary Methods**). This correlates with the temporal expression pattern of let-7, which begins to accumulate during the L3 stage[21]. As in this system let-7 expression is driven by a promoter that is active at all stages, but its effects are active only at later larval stages, these data may reflect a mechanism that regulates let-7 during development.

LIN-28 regulates pre–let-7 processing

Next we carried out forward genetic and RNA interference (RNAi) screens to identify factors that regulate let-7 activity *in vivo*. Knockdown of *lin-28* by RNAi resulted in reduced GFP expression at L1 and L2 stages, in a manner dependent on the *myo-2::let-7* transgene (**Supplementary Fig. 2a**,**b** and data not shown). We confirmed these results using a *lin-28* loss-of-function mutant (**Fig. 1e** and data not shown). Mutations in *lin-46* completely suppressed the developmental timing defect of *lin-28* mutants[22] but did not restore developmental regulation of let-7 (**Fig. 1e**). Thus, deregulation of let-7 activity in *lin-28* mutants is not an indirect consequence of developmental timing defects. Other heterochronic genes, including *lin-14* and *lin-42*, did not affect the let-7 sensor (**Supplementary Fig. 2c** and data not shown).

Next we tested whether LIN-28 was sufficient to inhibit let-7 activity. Ectopic expression of LIN-28 in the pharynx from an extrachromosomal array resulted in inhibition of let-7 in adults, which do not normally express LIN-28 (ref. 8)(**Fig. 1f**). Mosaic expression of the extrachromosomal array within the pharynx indicated that LIN-28 acts cell autonomously. We conclude that LIN-28 is required and sufficient to inhibit let-7 activity in *C. elegans*.

We then used miRNA microarrays and northern blotting to confirm that LIN-28 regulates endogenous let-7 accumulation in L2 larvae[23] (**Supplementary Fig. 3** and **Supplementary Data 1**). Furthermore, expression of other let-7 family members was not increased in *lin-28* mutants, whereas three unrelated miRNAs, including the developmentally regulated miRNA miR-85, showed increased expression in *lin-28* mutant L2s (**Supplementary Fig. 3a**,**b**).

Whether Lin28 regulates let-7 processing at the Drosha[15,16] or Dicer[17,18] step in mammalian cells is unresolved. We addressed this *in vivo* in *C. elegans*. We used northern blotting and quantitative reverse-transcription PCR (qRT-PCR) to compare expression of let-7 and its processing intermediates from the *myo-2::let-7* transgene in otherwise wild-type and *lin-28* mutant L2 larvae. *lin-28* mutants expressed higher levels of let-7 compared to the wild type, indicating increased processing efficiency; this was accompanied by a slight reduction in the level of pre–let-7, and no change in pri–let-7 levels; these data are consistent with increased efficiency of Dicer-mediated processing (**Supplementary Fig. 3c**,**d**). We obtained similar results for endogenous let-7, although levels of pri–let-7 were decreased in *lin-28* mutants, suggesting an indirect effect on the let-7 promoter (**Supplementary Fig. 3e**,**f**). Notably, miR-85 also seems to be regulated at the Dicer step in a *lin-28*–dependent fashion (**Supplementary Fig. 3b**,**g**). Consistent with these findings, a functional LIN-28-GFP translational fusion is localized in the cytoplasm[8] (**Supplementary Fig. 4a** and data not shown). Taken together, these data suggest that LIN-28 blocks Dicer-mediated processing of let-7 and possibly other developmentally regulated miRNAs.

Next, we tested whether LIN-28 directly interacts with pre–let-7. We performed pull-down assays using streptavidin beads and biotinylated pre–let-7. LIN-28-GFP from transgenic worm extracts was retained on streptavidin beads if the synthetic pre–let-7 RNA was biotinylated, but not using a non-biotinylated control (**Supplementary Fig. 4b**). We tested whether this interaction was direct by native gel mobility shift assay. pre–let-7 and GST–LIN-28 interact with an estimated K_d of 2 μM (**Supplementary Fig. 4c** and data not shown). We conclude that LIN-28 binds pre–let-7 to prevent Dicer processing. Experiments in mammalian cells suggested that the loop of the pre–let-7 hairpin is required for the interaction with Lin28 (refs. 15,24). However, the pre–let-7 loop is not conserved in *C. elegans*. We therefore tested a number of pre–let-7 loop mutants *in vivo* using the let-7 sensor. We found that the pre–let-7 loop is not required for the normal developmental regulation of let-7 activity (**Supplementary Fig. 5** and **Supplementary Methods**).

PUP-2 regulates pre–let-7 in a *lin-28*–dependent fashion

Our results so far were consistent with a LIN-28 blockade of pre–let-7 processing, but we were puzzled that pre–let-7 accumulation in L2 larvae differed little in wild-type compared to *lin-28* mutant animals (**Supplementary Fig. 3**). We reasoned that LIN-28 might target pre–let-7 for degradation. Recent work by Kim and colleagues demonstrated that Lin28 promotes pre–let-7 uridylation and subsequent degradation in mammalian cell lines, although the enzyme(s) involved are unknown[18]. We inspected published high-throughput sequencing data of *C. elegans* small RNA libraries[25,26] and found frequent modification

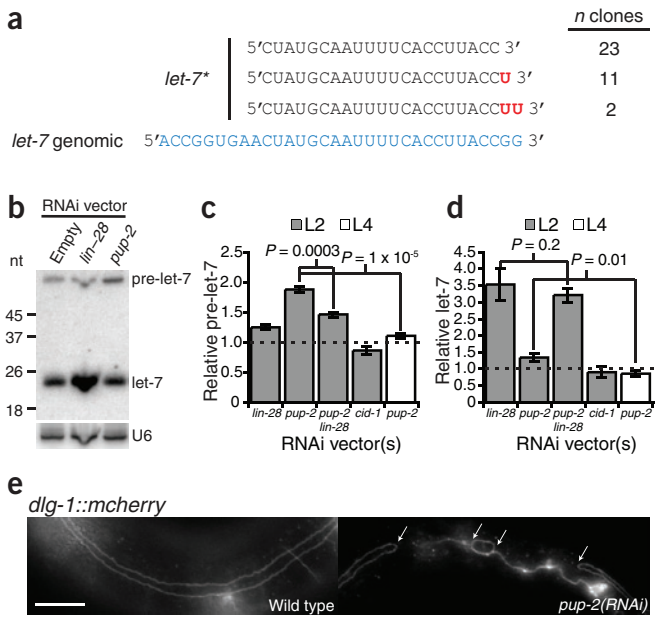

Figure 2 *pup-2* regulates let-7 processing in a *lin-28*–dependent fashion. (**a**) let-7 is uridylated *in vivo*. Frequency of unmodified and modified *let-7** molecules identified by high-throughput sequencing. (**b**) Representative northern blot showing *pup-2*–dependent regulation of pre–let-7, in which 5 µg of total RNA from control, *lin-28*(RNAi) and *pup-2*(RNAi) *myo-2::let-7* L2 larvae was loaded. U6 was used as a loading control. (**c**,**d**) Quantification of relative pre–let-7 (**c**) and let-7 (**d**) abundance in *lin-28*(RNAi), *pup-2*(RNAi) and *cid-1*(RNAi) *myo-2::let-7* L2 and L4 larvae from northern blotting experiments. Mean fold change relative to empty vector control samples is shown. *P*-values from Student's *t*-tests are indicated ($n = 4$). Error bars show s.e.m. (**e**) Fluorescence image showing the seam cell defect observed in *pup-2*(RNAi) adults. A DLG-1–mCherry fusion marks seam cell boundaries. Left, wild-type animal with a continuous seam; right, *pup-2*(RNAi) animals with incompletely fused seam. Arrows indicate sites of failed fusion. Scale bar shows 20 µm.

of the 3′ end of let-7* (3′ product of pre–let-7 processing) with one or two untemplated uracil residues (*C. elegans* let-7 resides on the 5′ arm of the hairpin; **Fig. 2a**). These species are likely to arise from Dicer processing of partially uridylated intermediates, and they indicate *in vivo* uridylation of let-7.

With this in mind, we carried out an RNAi screen against 15 potential poly(U) polymerases (**Supplementary Table 1**), assaying let-7 and pre–let-7 abundance in *myo-2::let-7* transgenic L2 larvae. RNAi against *pup-2* mRNA resulted in increased pre–let-7 levels (**Fig. 2b**,**c**; $P = 7.5 \times 10^{-5}$) and a small but significant increase in mature let-7 levels (**Fig. 2b**,**d**; $P = 0.029$). This effect is specific to *pup-2*; no other poly(U) polymerases, including *cid-1*, a potential paralogue, had this effect[27] (**Fig. 2c**,**d**). These data suggest that uridylation by PUP-2 targets pre–let-7 for degradation and is required for the maximally efficient blockade of let-7 processing by LIN-28.

We reasoned that LIN-28 might target uridylation of pre–let-7 by PUP-2, leading to degradation of the uridylated pre–let-7 and turnover of LIN-28–pre–let-7 complexes, ensuring efficient LIN-28 function. We examined the effect of *pup-2* RNAi in situations in which pre–let-7 is released from the LIN-28 blockade. The effect of *pup-2* RNAi on levels of both pre–let-7 and mature let-7 was abolished at the L4 stage (**Fig. 2c**,**d**; $P = 1 \times 10^{-5}$ and $P = 0.01$, respectively). Furthermore, L2 larvae exposed to both *pup-2* and *lin-28* RNAi show significantly reduced accumulation of pre–let-7 (**Fig. 2c**; $P = 0.0003$). These effects were not due to reduced RNAi against *pup-2* (**Supplementary Fig. 6a**). In contrast, the effect of *lin-28* RNAi on mature let-7 levels was not altered in L2 larvae subjected to *lin-28*, *pup-2* double RNAi (**Fig. 2d**; $P = 0.2$). From these data, we conclude that PUP-2 regulates let-7 post-transcriptionally in a LIN-28–dependent manner.

PUP-2 contributes to LIN-28-dependent regulation of let-7

Next we sought to determine whether PUP-2 is required for regulation of let-7 during development. Misregulation of let-7 results in altered timing of larval development, defects in differentiation of a hypodermal stem cell lineage required for the formation of adult-specific lateral alae[4] and defects in vulval morphogenesis[21]. Lateral seam cells differentiate and fuse into a syncytium in wild-type adults, but this fusion is defective if *pup-2* or *lin-28* is knocked down, consistent with a role in regulating let-7 (**Fig. 2e** and **Supplementary Table 2**). *pup-2* RNAi in a *lin-28* null mutant background did not increase seam cell fusion defects, suggesting that this activity of *pup-2* is *lin-28*–dependent (**Supplementary Table 2**).

Next we tested whether *pup-2* interacts genetically with let-7. For this we used *let-7*(*n2853*ts) mutant animals, which show reduced let-7 expression and temperature-sensitive vulval bursting[21]. At 15 °C, vulval bursting of *let-7*(*n2853*ts) animals was suppressed by *pup-2* RNAi, whereas *lin-28* RNAi suppressed vulval bursting at both 15 °C and 20 °C (**Table 1**). This weaker suppression of *let-7(n2853*ts) by *pup-2* compared to suppression by *lin-28* is consistent with a role for *pup-2* as a *lin-28* modifier at the genetic level. Taken together with the effect of *pup-2* on let-7 processing, these data indicate that *pup-2* ensures efficient activity of *lin-28* by targeting blockaded pre–let-7 molecules for destruction. This might occur via a LIN-28–dependent uridylyl-transferase activity of PUP-2 on pre–let-7, and we next sought to test this hypothesis *in vitro*.

PUP-2 uridylates pre–let-7 *in vitro*

We expressed hemagglutinin (HA)-Flag–tagged PUP-2 and Streptavidin binding peptide (SBP)-tagged LIN-28 in a HEK 293T human embryonic kidney cell line. Immunoprecipitation of HA-Flag–PUP-2 using anti-Flag antibodies specifically co-precipitated SBP–LIN-28 (**Fig. 3a**). This interaction occurred in the absence of *C. elegans* pre–let-7 and is therefore likely to be direct. Indeed, the addition of excess exogenous pre–let-7 to the cell extract did not enhance the interaction. We also confirmed this interaction in glutathione *S*-transferase (GST) pull-down experiments. *In vitro*–translated PUP-2 interacts directly with GST–LIN-28 (**Fig. 3b**).

PUP-2 was previously shown to polyuridylate an artificially tethered RNA in *Xenopus* oocytes but was inactive without tethering[27]. Therefore, we tested whether LIN-28 might be able to recruit PUP-2 to mediate pre–let-7 uridylation (**Fig. 3c**). We incubated anti-Flag immunoprecipitates from cell extracts expressing HA-Flag–PUP-2 and/or SBP–LIN-28 with radiolabeled pre–let-7 and radiolabeled UTP. HA-Flag–PUP-2 uridylated pre–let-7 only in the presence of SBP–LIN-28 (**Fig. 3c**). We also confirmed LIN-28–dependent uridylation of pre–let-7 by PUP-2 *in vitro* (**Supplementary Fig. 6b**). Finally, we attempted to identify *in vivo* uridylated pre–let-7 directly by cloning, but we were unable to

Table 1 Genetic interactions of *pup-2* and *lin-28* with *let-7* in vulval development

Genotype[a]	% burst at 20 °C (*n*)	% burst at 15 °C (*n*)
let-7(*n2853*); empty vector RNAi	97 (119)	47 (86)
let-7(*n2853*); *lin-28*(RNAi)	16 (115)	0 (28)
let-7(*n2853*); *pup-2*(RNAi)	97 (120)	28 (114)

[a]RNAi is by feeding.

do so. We conclude that rapid degradation of uridylated pre–let-7 prevents accumulation of these species *in vivo*, as has been postulated in human cell lines[18].

DISCUSSION

We have developed a quantitative assay of let-7 miRNA function in *C. elegans*. This assay is highly sensitive and amenable to high-throughput experiments. We have also isolated new mutants in known miRNA pathway components through mutagenesis screens using this assay (our unpublished data); analysis of novel miRNA function–defective mutants should provide insights into the mechanism of action of other miRNAs. In addition, this assay could be modified to study post-transcriptional regulation or target specificity of other miRNAs.

Here we demonstrate that LIN-28 regulates *C. elegans* pre–let-7 (see **Supplementary Fig. 7a** for a model). These results provide a molecular basis for the genetic link between *lin-28* and let-7 in controlling developmental timing. In *C. elegans*, this pathway determines the behavior of epithelial stem cells. In mammals, let-7 and Lin28 might regulate primordial germ cell differentiation and other stem cell lineages[28]. Therefore, the specific interaction of a structured RNA (pre–let-7) with a protein (Lin28) constitutes an ultraconserved switch regulating stem cell differentiation. The let-7 and *lin-28* switch might be as conserved as let-7 itself. For example, pre–let-7 processing is developmentally regulated in the sea urchin *Strongylocentrotus purpuratus*[13], which also expresses a Lin28 ortholog (data not shown).

Our finding that the terminal loop of pre–let-7 is dispensable for regulation by LIN-28 is at odds with two previous studies[15,16] but consistent with another involving competition experiments[17]. Our approach has been to assess let-7 function *in vivo*, whereas previous work was based on *in vitro* interaction studies. All 22 nucleotides of mature let-7 are conserved in bilateria, whereas for many other miRNAs only the 'seed' sequence (nucleotides 2–8) seems to be under evolutionary constraint. In contrast, there is little sequence similarity in the terminal loops of let-7 in different species. It is therefore tempting to speculate that nucleotides corresponding to mature let-7 contribute to LIN-28 recognition. Similar RNA-protein interactions might impose evolutionary constraint on the sequences of other ultraconserved miRNAs.

Here we show that LIN-28 recruits the poly(U) polymerase PUP-2 to uridylate *C. elegans* pre–let-7. We speculate that mammalian PUP-2 orthologs might similarly regulate let-7 in stem cells (**Supplementary Fig. 7b**). Indeed, the mouse Zcchc11 (also known as Tut4) uridylyl transferase regulates let-7 in embryonic stem cells[29]. let-7 is a candidate tumor suppressor[21,30–32], and LIN28 is a potential proto-oncoprotein[28,33]. Therefore, ZCCHC11 might be an important new target for anti-cancer therapy. Our data suggest that miRNAs are regulated through pre-miRNA sequestration and uridylation-dependent pre-miRNA degradation. This situation seems to be analogous to two-step regulation of the activity of proteins through sequestration and targeted degradation, for example, in the case of cadherin[34]. Uridylation-dependent degradation of RNA has been observed previously, and U tails have been shown to recruit either 5′-to-3′ or 3′-to-5′ exonucleases[35,36]. High-throughput sequencing suggests that other miRNAs and/or pre-miRNAs are subject to uridylation (data not shown), so regulation in this way may be widespread. Further uncovering the mechanisms underlying this pathway will be of great interest.

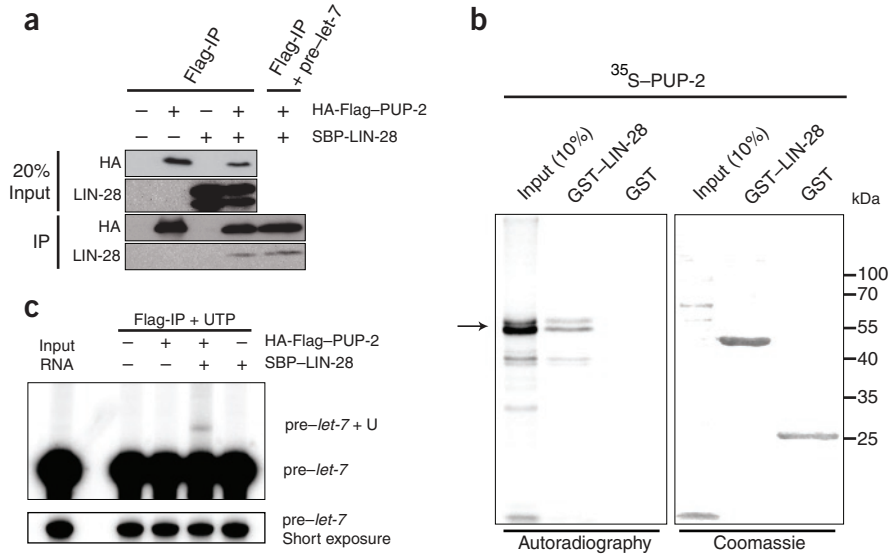

Figure 3 LIN-28 interacts with PUP-2 and promotes uridylation of pre–let-7 by PUP-2. (**a**) Co-immunoprecipitation (IP) of PUP-2 and LIN-28 expressed in HEK 293T cells. (**b**) GST pull-down assay demonstrating a direct interaction of GST–LIN-28 and PUP-2 *in vitro*. (**c**) *In vitro* uridylation assay showing that PUP-2 uridylates pre–let-7 in a LIN-28–dependent fashion.

METHODS

Methods and any associated references are available in the online version of the paper at http://www.nature.com/nsmb/.

Note: Supplementary information is available on the Nature Structural & Molecular Biology website.

ACKNOWLEDGMENTS

We thank A. Hutterer (Wellcome Trust Cancer Research UK Gurdon Institute, University of Cambridge) for a strain carrying the *mjIs15* transgene, M. Jackman (Wellcome Trust Cancer Research UK Gurdon Institute) for the pDEST-MAL, pcDNA5/FRT/TO_GATEWAY_TEV_SBP and pDEST-3Flag 3HA vectors, E. Moss (University of Medicine and Dentistry of New Jersey, USA) for anti–LIN-28 antibody and M. Wickens (University of Wisconsin, USA) for PUP-2 cDNA. We thank R. Gregory and N. Kim for sharing unpublished data. N.J.L. and K.J.M. were supported by a PhD studentship from the Wellcome Trust. J.A. and A.B. were supported by grants from the Biotechnology and Biological Sciences Research Council (UK). H.L.L. was supported by a PhD studentship from Cancer Research UK. This work was supported by Cancer Research UK Programme Grants to E.A.M. and S.B. and core funding to the Wellcome Trust/Cancer Research UK Gurdon Institute provided by the Wellcome Trust and Cancer Research UK.

AUTHOR CONTRIBUTIONS

N.J.L., S.B. and E.A.M. conceived the original project; N.J.L. carried out all experiments unless stated otherwise; J.A. carried out northern blotting, uridylase assays and microarray experiments; H.L.L., J.A. and A.B. carried out RNA mobility shift assays; K.J.M. and J.A. carried out some of the *in vitro* binding assays; N.J.L., J.A. and E.A.M. wrote the manuscript.

Published online at http://www.nature.com/nsmb.
Reprints and permissions information is available online at http://npg.nature.com/reprintsandpermissions/

1. Bartel, D.P. MicroRNAs: genomics, biogenesis, mechanism, and function. *Cell* **116**, 281–297 (2004).
2. Bartel, D.P. MicroRNAs: target recognition and regulatory functions. *Cell* **136**, 215–233 (2009).

3. Kim, V.N., Han, J. & Siomi, M.C. Biogenesis of small RNAs in animals. *Nat. Rev. Mol. Cell Biol.* **10**, 126–139 (2009).
4. Ambros, V. & Horvitz, H.R. Heterochronic mutants of the nematode *Caenorhabditis elegans*. *Science* **226**, 409–416 (1984).
5. Chalfie, M., Horvitz, H.R. & Sulston, J.E. Mutations that lead to reiterations in the cell lineages of *C. elegans*. *Cell* **24**, 59–69 (1981).
6. Lee, R.C., Feinbaum, R.L. & Ambros, V. The *C. elegans* heterochronic gene *lin-4* encodes small RNAs with antisense complementarity to *lin-14*. *Cell* **75**, 843–854 (1993).
7. Wightman, B., Ha, I. & Ruvkun, G. Posttranscriptional regulation of the heterochronic gene *lin-14* by *lin-4* mediates temporal pattern formation in *C. elegans*. *Cell* **75**, 855–862 (1993).
8. Moss, E.G., Lee, R.C. & Ambros, V. The cold shock domain protein LIN-28 controls developmental timing in *C. elegans* and is regulated by the *lin-4* RNA. *Cell* **88**, 637–646 (1997).
9. Slack, F.J. *et al.* The *lin-41* RBCC gene acts in the *C. elegans* heterochronic pathway between the let-7 regulatory RNA and the LIN-29 transcription factor. *Mol. Cell* **5**, 659–669 (2000).
10. Abrahante, J.E. *et al.* The *Caenorhabditis elegans* hunchback-like gene *lin-57*/*hbl-1* controls developmental time and is regulated by microRNAs. *Dev. Cell* **4**, 625–637 (2003).
11. Grosshans, H., Johnson, T., Reinert, K.L., Gerstein, M. & Slack, F.J. The temporal patterning microRNA let-7 regulates several transcription factors at the larval to adult transition in *C. elegans*. *Dev. Cell* **8**, 321–330 (2005).
12. Lin, S.Y. *et al.* The *C. elegans* hunchback homolog, *hbl-1*, controls temporal patterning and is a probable microRNA target. *Dev. Cell* **4**, 639–650 (2003).
13. Pasquinelli, A.E. *et al.* Conservation of the sequence and temporal expression of let-7 heterochronic regulatory RNA. *Nature* **408**, 86–89 (2000).
14. Winter, J., Jung, S., Keller, S., Gregory, R.I. & Diederichs, S. Many roads to maturity: microRNA biogenesis pathways and their regulation. *Nat. Cell Biol.* **11**, 228–234 (2009).
15. Newman, M.A., Thomson, J.M. & Hammond, S.M. Lin-28 interaction with the Let-7 precursor loop mediates regulated microRNA processing. *RNA* **14**, 1539–1549 (2008).
16. Viswanathan, S.R., Daley, G.Q. & Gregory, R.I. Selective blockade of microRNA processing by Lin28. *Science* **320**, 97–100 (2008).
17. Rybak, A. *et al.* A feedback loop comprising *lin-28* and let-7 controls pre-let-7 maturation during neural stem-cell commitment. *Nat. Cell Biol.* **10**, 987–993 (2008).
18. Heo, I. *et al.* Lin28 mediates the terminal uridylation of let-7 precursor MicroRNA. *Mol. Cell* **32**, 276–284 (2008).
19. Yu, J. *et al.* Induced pluripotent stem cell lines derived from human somatic cells. *Science* **318**, 1917–1920 (2007).
20. Miller, D.M., Stockdale, F.E. & Karn, J. Immunological identification of the genes encoding the four myosin heavy chain isoforms of *Caenorhabditis elegans*. *Proc. Natl. Acad. Sci. USA* **83**, 2305–2309 (1986).
21. Reinhart, B.J. *et al.* The 21-nucleotide let-7 RNA regulates developmental timing in *Caenorhabditis elegans*. *Nature* **403**, 901–906 (2000).
22. Pepper, A.S. *et al.* The *C. elegans* heterochronic gene *lin-46* affects developmental timing at two larval stages and encodes a relative of the scaffolding protein gephyrin. *Development* **131**, 2049–2059 (2004).
23. Bracht, J., Hunter, S., Eachus, R., Weeks, P. & Pasquinelli, A.E. Trans-splicing and polyadenylation of let-7 microRNA primary transcripts. *RNA* **10**, 1586–1594 (2004).
24. Piskounova, E. *et al.* Determinants of microRNA processing inhibition by the developmentally regulated RNA-binding protein Lin28. *J. Biol. Chem.* **283**, 21310–21314 (2008).
25. Das, P.P. *et al.* Piwi and piRNAs act upstream of an endogenous siRNA pathway to suppress Tc3 transposon mobility in the *Caenorhabditis elegans* germline. *Mol. Cell* **31**, 79–90 (2008).
26. Batista, P.J. *et al.* PRG-1 and 21U-RNAs interact to form the piRNA complex required for fertility in *C. elegans*. *Mol. Cell* **31**, 67–78 (2008).
27. Kwak, J.E. & Wickens, M. A family of poly(U) polymerases. *RNA* **13**, 860–867 (2007).
28. West, J.A. *et al.* A role for Lin28 in primordial germ-cell development and germ-cell malignancy. *Nature* **460**, 909–913 (2009).
29. Hagan, J.P., Piskounova, E. & Gregory, R.I. Lin28 recruits the TUTase Zcchc11 to inhibit let-7 maturation in mouse embryonic stem cells. *Nat. Struct. Mol. Biol.* advance online publication, doi:10.1038/nsmb.1676 (27 August 2009).
30. Johnson, C.D. *et al.* The let-7 microRNA represses cell proliferation pathways in human cells. *Cancer Res.* **67**, 7713–7722 (2007).
31. Johnson, S.M. *et al.* RAS is regulated by the let-7 microRNA family. *Cell* **120**, 635–647 (2005).
32. Yu, F. *et al.* let-7 regulates self renewal and tumorigenicity of breast cancer cells. *Cell* **131**, 1109–1123 (2007).
33. Chang, T.C. *et al.* Lin-28B transactivation is necessary for Myc-mediated let-7 repression and proliferation. *Proc. Natl. Acad. Sci. USA* **106**, 3384–3389 (2009).
34. Kowalczyk, A.P. & Reynolds, A.B. Protecting your tail: regulation of cadherin degradation by p120-catenin. *Curr. Opin. Cell Biol.* **16**, 522–527 (2004).
35. Mullen, T.E. & Marzluff, W.F. Degradation of histone mRNA requires oligouridylation followed by decapping and simultaneous degradation of the mRNA both 5′ to 3′ and 3′ to 5′. *Genes Dev.* **22**, 50–65 (2008).
36. Rissland, O.S. & Norbury, C.J. Decapping is preceded by 3′ uridylation in a novel pathway of bulk mRNA turnover. *Nat. Struct. Mol. Biol.* **16**, 616–623 (2009).

ONLINE METHODS

Nematode culture and strains. We grew *C. elegans* under standard conditions at 20 °C[37]. The food source used was *E. coli* strain HB101 (*Caenorhabditis* Genetics Center, University of Minnesota). We used bleaching followed by starvation-induced L1 arrest to generate synchronized cultures. The wild-type strain was var. Bristol N2[38]. Additional strains used are listed in **Supplementary Table 3**.

DNA constructs and transgenics. We generated DNA vectors using the Multisite Gateway Three-Fragment vector construction kit (Invitrogen) (**Supplementary Data 2**). We performed site-directed mutagenesis using PCR and mutagenic primers (**Supplementary Data 2**). All constructs were confirmed by sequencing. To generate transgenic animals, we performed germline transformations as described[39]. Injection mixes contained 2–10 ng μl^{-1} of vector, 5–10 ng μl^{-1} of marker and the Invitrogen 1-kb ladder to a final concentration of 100 ng μl^{-1} DNA (see **Supplementary Methods** for details). We integrated array transgenes via X-ray irradiation as described[40]. We generated single-copy transgenes by transposase-mediated integration (mosSCI) as described[41].

Microscopy. We carried out differential interference contrast (DIC) and fluorescence imaging by standard methods[42] using an AxioImager A1 upright microscope (Zeiss). We captured images using an ORCA-ER digital camera (Hamamatsu) and processed them using OpenLabs 4.0 software (Improvision). For analysis of let-7 sensor transgene expression, we imaged all animals under identical conditions. We performed confocal microscopy using an Olympus FluoView FV1000 upright microscope using 63× objective magnification.

Analyses with the COPAS Biosort instrument. We used a COPAS Biosort instrument (Union Biometrica) to simultaneously measure length (time of flight), absorbance (extinction) and fluorescence. We optimized fluorophore detection for simultaneous detection of GFP and mCherry. We used a multiline solid-state argon laser for excitation (488 nm for GFP and 561 nm for mCherry) and detected emission by appropriate PMTs (photomultiplier tubes) after passing through band pass filters (510/23 nm for GFP and 615/45 nm for mCherry). We harvested animals from plates and washed them in M9 buffer[37] before sorting. We determined length and absorbance for each larval stage using synchronized wild-type populations. We then generated gates to isolate animals of specific developmental stages from mixed populations (**Supplementary Fig. 1a**).

RNA interference assays. We obtained RNAi clones from genome-wide RNAi libraries[43–45]. We generated additional RNAi constructs by subcloning of an appropriate genomic DNA fragment into pDEST-L4440[45,46] (**Supplementary Data 2**). We confirmed all RNAi constructs by sequencing. For experiments using let-7 sensor and *myo-2::let-7* transgenes, we performed RNAi by feeding, as described, using the *eri-1*(*mg366*) RNAi hypersensitive genetic background[47]. For COPAS Biosort analysis, we plated 10–50 L1 larvae on 90-mm RNAi plates and analyzed the animals once the oldest progeny reached the L3 larval stage. For harvest and RNA extraction, we plated ~3,000 L1 larvae per RNAi plate and grew the animals to adulthood before bleaching. After synchronization by starvation, we plated the progeny onto fresh RNAi plates and grew them to the desired stage before harvesting. We performed RNAi by injection as described[48]. We analyzed phenotypes on progeny laid 24–48 h post-injection.

Phenotypic analysis of seam cell development. We performed RNAi by injection into strains carrying seam cell marker transgenes *wIs51* and *mjIs15*.

Vulval bursting assay. We added *let-7*(*n2853*ts) embryos to RNAi plates by bleaching gravid adults, and we grew them at 15 °C. Non-burst adults were then transferred to fresh RNAi plates and temperature-shifted as required. L4 progeny were picked to fresh RNAi plates (15–25 animals per plate), and vulval bursting was scored after 48 h.

RNA extraction. For total RNA isolation we harvested animals from plates by washing with M9 (ref. 37). We pelleted and froze the animals in liquid nitrogen and then dissolved the pellets in 10 volumes of Trizol reagent (Invitrogen). We extracted total RNA using Trizol reagent according to the manufacturer's protocol.

miRNA microrarray analysis. We performed miRNA microarrays using custom DNA oligonucleotide arrays, as described[49,50]. Data analysis was as described[50]. To compare miRNA expression in wild-type and *lin-28* mutant L2 larvae, we isolated and size-selected total RNA from synchronized animals to 18–26 nt using PAGE. The small RNA fraction was 3′ end labeled using T4 RNA ligase (Fermentas UK). *C. elegans* miRNA microarrays were based on miRbase release 8.0 (refs. 51,52). We performed all experiments in triplicates. For microarray probe information and primary microarray data see **Supplementary Data 1**.

Northern blotting. We performed northern blotting as described[25,53], with the following modifications. We used 5–20 µg total RNA, or the small RNA fraction (miRvana, Ambion) isolated from ~200 µg total RNA. For developmental expression profiles (**Supplementary Fig. 3a**) we carried out 1-ethyl-3-[3-dimethylaminopropyl]carbodimide hydrochloride (EDC, Perbio Science) cross-linking reactions for 2 h at 60 °C. Otherwise, blots were UV cross-linked. We modified northern hybridizations as follows: membranes were prehybridized at 40 °C for 4 h in hybridization buffer (0.36 M Na_2HPO_4, 0.14 M NaH_2PO_4, 7% (v/v) SDS and 1 mg of sheared, denatured salmon sperm DNA) and hybridized at 40 °C overnight using 20 pmol of γ-^{32}P-ATP–radiolabeled DNA oligonucleotide probes (**Supplementary Data 2**). After hybridization, we washed the membranes twice with 0.5× SSC, 0.1% (v/v) SDS at 40 °C for 10 min and once with 0.1× SSC, 0.1% (v/v) SDS at 40 °C for 5 min. We detected radioactivity by PhosphorImager (GE Healthcare). We quantified band intensity using ImageQuant software (GE Healthcare).

Real-time RT-PCR. We performed RT-PCR as described[25], using the standard curve method. Primers used are listed in **Supplementary Data 2**.

Pre–let-7 pull-down. For these experiments we generated a strain carrying a rescuing *lin-28::gfp* translational fusion transgene (mosSCI integrated) in a *lin-28*(*n719*) mutant background. We prepared protein extracts from starvation-synchronized L1 larvae. We cleared lysates against Streptavadin Dynabeads (Invitrogen) for 30 min at 4 °C in PD buffer (18 mM HEPES-KOH, pH 7.9, 10% (v/v) glycerol, 40 mM KCl, 2 mM $MgCl_2$, 10 mM DTT, 100 µM $ZnSO_4$, 1× Proteinase Inhibitor Cocktail (PIC; Roche)). Dynabeads were blocked with 15 µg yeast tRNA for 1 h at 4 °C in PD buffer before addition of 100 pmol synthetic 5′ biotinylated pre–let-7 (Microsynth) for pull-down, or unmodified synthetic pre–let-7 for control reactions, and incubated for 1 h at room temperature. We added preblocked Dynabeads to the binding reaction and incubated for 1 h at room temperature (24 °C). We washed the beads three times in PD buffer. We analyzed bound proteins by western blotting with primary mouse anti-GFP (Clontech JL-8; 1:1,000) and secondary horseradish peroxidase (HRP)-conjugated anti-mouse (Dakocytomation P0450; 1:10,000), or rat anti-tubulin (Chemicon international MAB1684, 1:1,000) and secondary HRP-conjugated mouse anti-rat (GE Healthcare NA9310; 1:10,000).

Recombinant protein expression. We obtained LIN-28 cDNA (F02E9.2b) from the ORFeome library[45]. We subcloned cDNAs into pDEST-GEX-2TK (Gateway cassette inserted at SmaI site in pGEX-2TK), or pDEST-MAL. We expressed and purified recombinant proteins as described[25,54].

GST pull-down. We used PUP-2 cDNA in pDEST14 (Invitrogen) to produce ^{35}S-methionine–radiolabeled protein by *in vitro* transcription translation using a TNT T7–coupled reticulocyte lysate kit (Promega). We performed pull-downs using GST-LIN-28, as described[54].

Pre–let-7 transcription. We performed *in vitro* transcription reactions in a volume of 20 µl with a 0.5 mM concentration of each NTP, 40 mM Tris, pH 7.9, 12 mM $MgCl_2$, 2 mM spermidine, 20 mM DTT, 1 mM NaCl, 100 U T7 RNA polymerase (Roche) and 1U RNasin (Promega). We incubated reactions for 1 h at 37 °C, before phenol-chloroform extraction and ethanol precipitation. We transcribed radiolabeled RNA for electrophoretic mobility shift assays with α-^{32}P-UTP to a specific activity of approximately 6,000 cpm $fmol^{-1}$.

Immunoprecipitation. We cloned LIN-28 cDNA into pcDNA5/FRT/TO_GATEWAY_TEV_SBP. We cloned PUP-2 cDNA into pDEST-3Flag 3HA. We performed immunoprecipitation assays as described[18]. Briefly, we transfected HEK 293T cells with pHA-Flag-PUP-2 and/or pLIN-28-SBP. After 48 h, we

collected cells in cold lysis buffer (500 mM NaCl, 1 mM EDTA, 10 mM Tris, pH8.0, 1% (v/v) Triton X-100), sonicated for 4 min on ice and centrifugated for 10 min. We incubated 50 µl of the supernatant was with 5 µl of prewashed anti-Flag antibody, conjugated to agarose beads (Sigma) and incubated for 2 h at 4 °C. We washed the agarose beads twice with lysis buffer and twice with buffer D. For *in vitro* uridylation, we incubated agarose beads in a 30-µl reaction containing 3.2 mM $MgCl_2$, 1 mM DTT and 0.25 mM rUTP and 5′ end–labeled pre-miRNA of 1×10^4 cpm to 1×10^5 cpm, for 20 min at 37 °C. We purified RNA by Trizol extraction and isopropanol precipitation. We analyzed reactions in a 12% urea polyacrylamide gel.

***In vitro* uridylation assays.** We performed *in vitro* uridylation assays in 30-µl reactions containing 1.5 µg of *in vitro*–transcribed pre–let-7 in 10 mM Tris, pH 7.5, 30 mM KCl, 1 mM DTT, 10 mM $MnCl_2$, 2 mM $MgCl_2$, 0.25 mM UTP, 1 µl of RNaseOut and 0.01 Mbq α-^{32}P-UTP. We added 1 µg of recombinant MBP–PUP-2 and increasing amounts of recombinant GST–LIN-28 to a maximum of 10 µg. We incubated reaction mixtures at 30 °C for 30 min. We purified RNA by phenol-chloroform extraction and ethanol precipitation. We analyzed reactions in a 6% urea polyacrylamide gel. We used 2 U of *Schizosaccharomyces pombe* CID1 poly(U) polymerase (NEB) as a positive control. We detected radioactivity by PhosphorImager (GE Healthcare).

Electrophoretic mobility shift assay. We carried out binding reactions in a total volume of 20 µl containing 50,000 cpm of radiolabeled RNA, 30 µg tRNA, 1 µl RNaseOut (40 U μl^{-1}) (Invitrogen), 50 mM Tris, pH 7.6, 100 mM NaCl, 0.07% (v/v) β-mercaptoethanol, 5 mM magnesium acetate and increasing amounts of recombinant GST–LIN-28 to a maximum of 10 µM. We incubated the reactions at room temperature for 45 min, followed by analysis using 5% native PAGE. We detected radioactivity by PhosphorImager (GE Healthcare).

37. Wood, W. *The Nematode Caenorhabditis elegans.* (Cold Spring Harbor Press, Cold Spring Harbor, NY, 1988).
38. Brenner, S. The genetics of *Caenorhabditis elegans. Genetics* **77**, 71–94 (1974).
39. Mello, C. & Fire, A. DNA transformation. *Methods Cell Biol.* **48**, 451–482 (1995).
40. Fire, A. Integrative transformation of *Caenorhabditis elegans. EMBO J.* **5**, 2673–2680 (1986).
41. Frøkjær-Jensen, C. *et al.* Single-copy insertion of transgenes in *Caenorhabditis elegans. Nat. Genet.* **40**, 1375–1383 (2008).
42. Horvitz, H.R. & Sulston, J.E. Isolation and genetic characterization of cell-lineage mutants of the nematode *Caenorhabditis elegans. Genetics* **96**, 435–454 (1980).
43. Fraser, A.G. *et al.* Functional genomic analysis of *C. elegans* chromosome I by systematic RNA interference. *Nature* **408**, 325–330 (2000).
44. Kamath, R.S. *et al.* Systematic functional analysis of the *Caenorhabditis elegans* genome using RNAi. *Nature* **421**, 231–237 (2003).
45. Rual, J.F. *et al.* Toward improving *Caenorhabditis elegans* phenome mapping with an ORFeome-based RNAi library. *Genome Res.* **14**, 2162–2168 (2004).
46. Timmons, L., Court, D.L. & Fire, A. Ingestion of bacterially expressed dsRNAs can produce specific and potent genetic interference in *Caenorhabditis elegans. Gene* **263**, 103–112 (2001).
47. Kennedy, S., Wang, D. & Ruvkun, G. A conserved siRNA-degrading RNase negatively regulates RNA interference in *C. elegans. Nature* **427**, 645–649 (2004).
48. Fire, A. *et al.* Potent and specific genetic interference by double-stranded RNA in *Caenorhabditis elegans. Nature* **391**, 806–811 (1998).
49. Miska, E.A. *et al.* Microarray analysis of microRNA expression in the developing mammalian brain. *Genome Biol.* **5**, R68 (2004).
50. Wienholds, E. *et al.* MicroRNA expression in zebrafish embryonic development. *Science* **309**, 310–311 (2005).
51. Griffiths-Jones, S. The microRNA Registry. *Nucleic Acids Res.* **32**, D109–D111 (2004).
52. Griffiths-Jones, S., Grocock, R.J., van Dongen, S., Bateman, A. & Enright, A.J. miRBase: microRNA sequences, targets and gene nomenclature. *Nucleic Acids Res.* **34**, D140–D144 (2006).
53. Pall, G.S. & Hamilton, A.J. Improved northern blot method for enhanced detection of small RNA. *Nat. Protoc.* **3**, 1077–1084 (2008).
54. Sapetschnig, A. *et al.* Transcription factor Sp3 is silenced through SUMO modification by PIAS1. *EMBO J.* **21**, 5206–5215 (2002).

doi:10.1038/nsmb.1675